Residual Stresses in Functionally Graded Thermal Barrier Coatings

Abir Bhattacharyya*, David Maurice

U.S. Department of Energy, National Energy Technology Laboratory,
1450 Queen Ave SW, Albany, OR 97321, USA

ABSTRACT

Functionally graded materials offer potential as a solution to the premature failure of thermal barrier coatings due to thermal residual stresses, however this solution has not been fully evaluated to date. An analytical methodology based on the bending of plates has been used to model the residual stress distribution through the layers of a functionally graded (FG) cermet top coat-bond layer-substrate system after cooling from a high deposition temperature. The model is then applied to two material systems with different trends in variation in the coefficient of thermal expansion from the substrate to the top coat layer. Increasing the number of layers reduces the discrete stress variations across the interfaces through the FG layers and reduces the propensity of interfacial cracking. While the stress in the top coat is always compressive for the Inconel substrate, the stress in the top coat is tensile in nature for the steel substrate when the ceramic volume fraction in the functionally graded layers is low. The stress in the top coat gradually becomes compressive with an increasing volume fraction of ceramic in the functionally graded top coat. The curvature of the TBC system follows a similar trend and changes its sign with increasing ceramic content for the steel substrate. The effect of the number of layers on the curvature gradually diminishes and the curvature becomes constant beyond only a few layers.

Keywords: Thermal barrier coatings, functionally graded material, residual stresses, thermal stress

1. INTRODUCTION

Thermal barrier coatings (TBCs) are refractory-based films that are used to protect a metallic component from high temperature exposure [1-4]. A typical TBC system consists of three layers, (i) the TBC or a top coat, (ii) a bond coat which is typically an environmental barrier layer between the top coat and the metallic component and (iii) a metallic substrate. The top coat is usually a ceramic based material, which provides thermal protection to the substrate [5]. A typical TBC is expected to have a high melting point, low thermal conductivity, chemical inertness, a thermal expansion coefficient similar to that of the substrate, and no phase transformation between the room temperature and operating temperature [5, 6]. The bond coat layer provides protection of the substrate by preventing interactions with the reaction chamber environment in the event of partial or complete breakdown of the TBC.

The adherence of the interfaces between different layers of a thermal protection system depends upon the materials pairing and upon the processing used to join them. The quality and performance of a TBC strongly depends on top coat-bond coat and bond coat-substrate adhesion characteristics [7]. Although a sufficiently strong adherence is generally obtained between the metallic substrate and the bond coat, the interfacial adhesion can be weak between the bond coat and the TBC due to difficulty in obtaining a strong metal-ceramic bonding across the interface [8]. A strong chemical bonding between metal and ceramic is influenced by the surface energies of metal and ceramic, the interfacial energy and work of adhesion, the orientation relationship between crystal lattices across the ceramic/metal interface, and the segregation of atoms at the metal/ceramic interface [8, 9]. However, the requirements of the high temperature resistance, low

thermal conductivity, strength and abrasion resistance ability of the components narrows down the choice of TBC materials [10, 11]. Similarly, the choice of the bond coat material is limited by the requirements of minimal difference in the coefficients of thermal expansion between the TBC and metallic substrate, and of resistance to chemical attack by forming a protective layer [12].

Failure of a TBC might occur either by cracking within the ceramic top coat or by cracking at the top coat-bond coat interface [13, 14]. High stresses can be generated within the ceramic in the vicinity of the interface due to thermal mismatch and lattice misfit between the TBC and bond coat. Lattice misfit can either lead to high stress or can generate defects at the TBC-bond coat interface [14, 15]. Failure will occur at the interface if the interface is weaker than the ceramic itself. The defects due to lattice misfit between the TBC and the bond coat reduces the adhesion of the interface and facilitates interfacial delamination. However, the effect of lattice misfit on the stresses through the TBC layers is limited to only a small thickness of 100-200 nm. Beyond that thickness, the thermal mismatch between the TBC layers plays the dominant role in governing the failure of the TBC system [15].

During the deposition and thermal cycling processes, thermal barrier coatings (TBCs) deposited by plasma spraying and physical vapor deposition were prone to premature failure because of thermal residual stresses due to high thermal expansion mismatches among the coating layers and substrate [16]. Deposition of these coatings by laser additive manufacturing is also expected to be a problem as a high temperature is involved in the deposition by melting and solidification processes. Functionally graded materials, which are essentially multilayered systems (described in section 2), offer potential as an effective solution, as they reduce the difference in the CTE and lattice parameter mismatch between the consecutive layers [17-19].

Thermal stresses in multilayered elastic systems have been modelled previously [20-24]. For a typical TBC system with a uniform top coat, bond coat, and substrate, an analytical solution for thermal stresses is not very complex and a closed-form solution is available in literature [25]. But with the increasing number of layers in the system, and the displacement compatibility condition at interfaces between layers to be satisfied, the complexity in obtaining a closed-form solution increases. Therefore, most of the analyses, except that by Hsueh [26] and Zhang et al.[27], consider simplified assumptions (e.g. a constant Young's modulus throughout the system) to obtain closed-form solutions or are solved numerically by computer [21, 23, 24]. The effects of substrate material, number of functionally graded layers, the volume fraction of ceramics in the top coat on the stress profile and the geometry and curvature of the TBC system have not been investigated through modeling before. Therefore, it is necessary to address these effects through an analytical model.

In this effort, we use the bending theory of plates to model the residual stress through the functionally graded TBC system. We have selected two different TBC-substrate material systems to compare the residual stress distribution through the layers after the deposition of the TBC. The substrate materials in the two material systems are Inconel 718 (IN 718) and A516 pressure vessel steel, respectively. In the first case, on the IN718 we assume the deposition of a NiCrAlY bond coat layer, and on that the deposition of partially stabilized Yittria stabilized zirconia (YSZ). In the second case, on an A516 pressure vessel steel we assume the deposition of a 100% Inconel 625 bond coat layer, and on that the deposition of a functionally graded cermet of PSZ and Inconel 625.

For both cases the residual stresses developed due to the deposition and subsequent cooling from the deposition temperature to the room temperature are modeled analytically. The

interfacial stresses are estimated after incorporating the effects of thermal mismatch between adjacent layers. The coating thickness-dependent Young's modulus variation is incorporated in the model to capture the discrete stress profiles at the functionally graded layers. It is shown that the deposition temperature, mismatch in the coefficient of thermal expansion, numbers of graded layers and the volume fraction of the YSZ ceramic within the cermet top coat are critical to the manufacturing of thermal protection system for engineering components.

2. ANALYTICAL MODEL

A functionally graded (FG) coating material is characterized by varying physical and mechanical properties due to changes in composition along its dimensions. A schematic of a typical functionally graded TBC system is shown in Fig. 1. For building the model we consider a material A as a bond coat deposited on the substrate. The top coat is a functionally graded material which is assumed to be a homogeneous mixture of material A and a material B with varying concentration through the depth. The physical and mechanical properties are varied by a stepwise change in composition from 100% A to a mixture of materials A and B through n number of layers. The thickness of each layer is denoted by t_i. The thickness of the substrate is t_s. The interface between the substrate and the layer above it is defined as the $z = 0$. The total thickness of the coating, h_i is the summation of individual layer thicknesses and can be defined as $h_i = \sum_{j=1}^{i} t_j$. The thickness of substrate is t_s.

In this model, the Young's modulus (E) of each individual layer of the FG coating with the increasing number of layers is expressed by Vegard's rule as,

$$E = E_A V_A + E_B V_B \tag{1}$$

where $V_B = 1 - V_A$ and E_A and E_B are the Young's modulus of material A and B, respectively. The coefficient of thermal expansion (α) for each layer can similarly be expressed as

$$\alpha = \alpha_A V_A + \alpha_B V_B \tag{2}$$

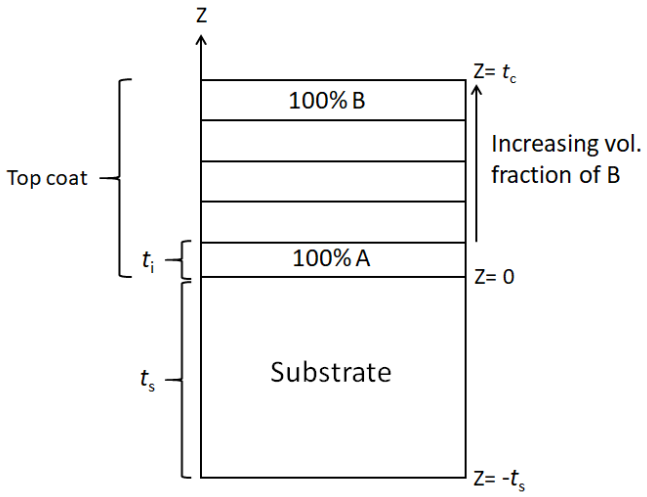

Figure 1: Schematic of a TBC system with functionally graded top coat. The first layer above the substrate has 100% of material A. The volume fraction of a material B increases with each additional layer of the top coat.

We assume that the whole coating system is cooled from a stress-free state. The thermal strain during cooling due to the difference in coefficient of thermal expansion between substrate and the TBC layers is expressed as,

$$\Delta\varepsilon = (\alpha_s - \alpha_i)\Delta T \tag{3}$$

Where α_s and α_i are the coefficient of thermal expansion of the substrate and layer i of the TBC, and ΔT is the temperature difference between the deposition temperature and room temperature.

In-plane forces will be generated in the film and the substrate due to thermal mismatch strain between the layers. The thermal mismatch strain in each layer can be expressed as

$$\Delta\varepsilon = \frac{F_i}{E_i t_i} - \frac{F_s}{E_s t_s} \tag{4}$$

Where E_s and E_i are the Young's modulus and F_s and F_i are the in-plane force uniformly distributed across the substrate and the i th layer of the film, respectively.

According to the force equilibrium condition, $\sum F_i + F_s = 0$ (5)

By combining Eq. (3) -(5), the strains in each layer of the film and in the substrate can be expressed as

$$F_i = \frac{E_i t_i \left[E_s t_s \Delta\alpha \Delta T + \sum_{k=1}^{n} E_k t_k (\alpha_k - \alpha_i) \Delta T \right]}{\sum_{i=1}^{n} E_i t_i + E_s t_s} \tag{6}$$

$$F_s = \frac{-E_s t_s \sum_{i=1}^{n} E_i t_i \Delta\alpha \Delta T}{\sum_{i=1}^{n} E_i t_i + E_s t_s} \tag{7}$$

And the strain in the i th layer and in the substrate can be expressed as

$$\varepsilon_i^{\,0} = \frac{E_s t_s \Delta\alpha \Delta T + \sum_{k=1}^{n} E_k t_k (\alpha_k - \alpha_i) \Delta T}{\sum_{i=1}^{n} E_i t_i + E_s t_s} \tag{8}$$

$$\varepsilon_s^{\,0} = \frac{-\sum_{i=1}^{n} E_i t_i \Delta\alpha \Delta T}{\sum_{i=1}^{n} E_i t_i + E_s t_s} \tag{9}$$

A bending strain arises due to the bending moment of the whole system and needs to be accounted for via total stress calculations. The bending strain can be expressed as

$$\varepsilon(k) = K(z+\delta),\ -t_s \le z \le t_c \tag{10}$$

where δ is the distance from the bending axis to the interface between the substrate and the first layer (i.e. $z=0$), and K is the curvature.

Now we apply force and moment equilibrium on this system. From Force equilibrium,

$$\int_{-t_s}^{0} KE_s(z+\delta)dz + \sum_{i=1}^{n}\int_{h_{i-1}}^{h_i} KE_i(z+\delta)dz = 0 \tag{11}$$

From moment equilibrium,

$$\int_{-t_s}^{0} KE_s(z+\delta)^2 dz + \sum_{i=1}^{n}\int_{h_{i-1}}^{h_i} KE_i(z+\delta)^2 dz = M \tag{12}$$

This bending moment should be balanced by the moments from the in-plane forces, F_i and F_s and the sum of the moments with respect to the bending axis will be zero.

$$M + \int_{-t_s}^{0} \frac{F_s}{t_s}(z+\delta)dz + \sum_{i=1}^{n}\int_{h_{i-1}}^{h_i} \frac{F_i}{t_i}(z+\delta)dz = 0 \tag{13}$$

Combining Eqs. (11)-(13), we determine the expressions for δ, M and K as

$$\delta = \frac{E_s {t_s}^2 - \sum_{i=1}^{n} E_i t_i (2h_{i-1} + t_i)}{E_s t_s + \sum_{i=1}^{n} E_i t_i} \tag{14}$$

$$M = \frac{KE_s t_s}{3}\left[3t_s\delta^2 - 3{t_s}^2\delta + {t_s}^3\right] + K\sum_{i=1}^{n}\frac{E_i t_i}{3}\left[3t_i {h_{i-1}}^2 + 3h_{i-1}{t_i}^2 + {t_i}^3 + 3t_i\delta^2 + 3\delta(2t_i h_{i-1} + {t_i}^2)\right] \tag{15}$$

$$K = -\frac{\left\{3\sum_{i=1}^{n} E_i t_i (2h_{i-1} + t_i)\left[E_s t_s \Delta\alpha\Delta T + \sum_{k=1}^{n} E_k t_k (\alpha_k - \alpha_i)\Delta T\right] + 3E_s t_s \sum_{i=1}^{n} E_i t_i t_s \Delta\alpha\Delta T\right\}}{\left\{2E_s t_s\left[3\delta^2 - 3t_s\delta + {t_s}^2\right] + \sum_{i=1}^{n} 2E_i t_i\left[3{h_{i-1}}^2 + 3h_{i-1}t_i + {t_i}^2 + 3\delta^2 + 3\delta(2h_{i-1} + t_i)\right]\right\}\left(\sum_{i=1}^{n} E_i t_i + E_s t_s\right)} \tag{16}$$

The stresses in individual layers of the film (σ_i) and in the substrate (σ_s) are now calculated as

$$\sigma_i = E_i\left[\varepsilon_i^0 + K(z+\delta)\right],\ 1 \le i \le n,\ h_{i=1} \le z \le h_i \tag{17}$$

$$\sigma_s = E_s\left[\varepsilon_s^0 + K(z+\delta)\right],\ -t_s \le z \le 0 \tag{18}$$

3. MATERIALS AND PROPERTIES

Two different TBC systems, representative as systems of interest for functionally gradients TBCs, are analyzed through this model. The bond coat material is material A in the schematic of Fig. 1. The ceramic material used in the top coat cermet is material B in Fig.1. TBC system 1 (S-1) is typical of that used in turbine blades of aerospace engines, which consists of Inconel 718 substrate, an MCrAlY bond coat and a functionally graded cermet top coat of MCrAlY and partially stabilized YSZ. The partially stabilized zirconia fraction is increased with increasing coating thickness. TBC system 2 (S-2) consists of a steel substrate made of a pressure vessel type steel A516, an Inconel 625 bond coat and a functionally graded cermet top coat of Inconel 625 and partially stabilized YSZ. S-2 may be an appropriate TBC system for the inner liners of a furnace or a reactor. The material properties are provided in Table 1.

Table 1: Young's modulus and coefficient of thermal expansion of YSZ ceramic, bond coat and substrate materials

Material	***E* (GPa)**	**α (10^{-6}/K)**
YSZ (ZrO2, 8 YSZ)	80 GPa	8.6
MCrAlY (M= Ni)	170 GPa	12.5
Inconel 625	208 GPa	13.1
Inconel 718	204 GPa	14.4
A516	204 GPa	12

The coefficient of thermal expansion (CTE) gradually decreases from the substrate to the top coat for S-1, whereas the CTE increases first from the substrate to the bond coat and then decreases as the YSZ volume fraction is increased in the top coat.

4. RESULTS AND DISCUSSION

The thickness values of the bond coat and the substrate are kept constant at 0.2 mm (200 μm) and 12.7 mm, respectively, for both systems. The substrate, bond coat and top coat are assumed to be stress-free at a deposition temperature of 1025°C, which leads to a temperature difference of $\Delta T = (25 - 1025)$ °C = -1000°C upon cooling.

The stress profiles of TBC systems S-1 and S-2 upon cooling by $\Delta T = 1000$°C are shown in Fig. 2(a) and 2(b). Three layers of gradation are considered in both the cases. The YSZ volume fraction is increased to 1%, 5% and 10% in subsequent 0.6 mm layers, leading to the

total top coat thickness of 1.8 mm. Such thick coatings are necessary for typical temperature reductions between 200 °C and 400°C through the top coat during high-temperature operation of turbine blades. The top coat is subjected to compressive elastic stresses upon cooling in S-1 (Fig. 2). The magnitude of stress increases with increasing the YSZ fraction towards the surface. Sharp and discrete stress drops occur at the interfaces of the functionally graded top coat. The maximum stress drop (148 MPa to -200 MPa) occurs at the interface between the IN718 substrate and the MCrAlY bond coat. The stress drop continues to occur through the functionally graded layers and finally reduces to -229 MPa at the free surface at 2 mm above the substrate-bond coat interface. The stress drops at the interfaces of the functionally graded coating are significantly smaller in magnitude (-206 MPa to -238 MPa at the 1.4 mm depth from the IN 718 substrate-MCrAlY bond coat interface) and the compressive stress reduces from -238 MPa to -229 MPa at the free surface through the third functionally graded layer.

The sharp stress drop at the IN 718-MCrAlY interface is due to the large difference in the coefficients of thermal expansion of the respective materials (Table 1). The IN 718 substrate is subjected to a small elastic tensile stress of 148 MPa (yield strength of IN 718 is ~1.1 GPa). In contrast, the profile for TBC system S-2 shows that the substrate is subjected to a small compressive stress of -70 MPa and the subsequent layers are subjected to tensile stress. The maximum tensile stress of 157 MPa exists at the substrate-IN 625 interface. Therefore, instead of a stress drop (as in S-1), a stress jump is predicted at the substrate-bond coat interface in S-2. The IN 625 bond coat (yield strength= 63 MPa and ultimate tensile strength= 132 MPa) is supposed to plastically yield and may even fail at such high stress level. However, the stress within the top coat decreases with increasing YSZ volume fraction with the increasing thickness, and reduces to 43 MPa at the free surface at 2 mm above the A516 steel substrate-IN 625 interface.

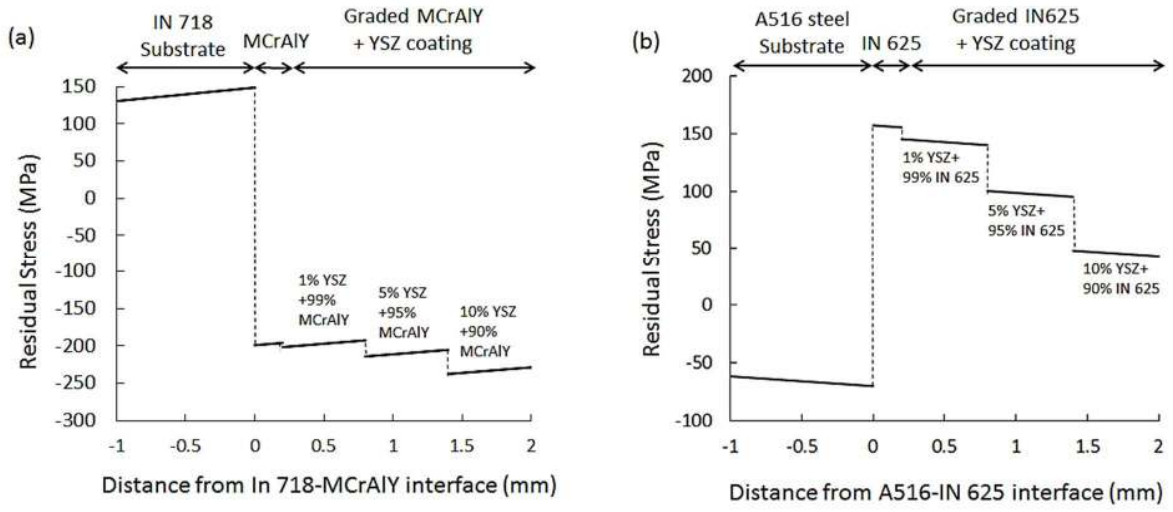

Figure 2: Residual stress profiles for (a) IN 718-MCrAlY+YSZ (S-1) and (b) A516-IN 625+YSZ (S-2) TBC system. The film is under compression and the substrate is under tension for S-1, whereas the film is under tension and the substrate is under compression for S-2.

A similar stress profile was predicted by Zhang et al.[27] for a functionally graded TBC system with a ZrO_2-Y_2O_3+NiCrAlY FG top coat layer on various Inconel substrates. However, with the temperature difference, ΔT being only 400°C in their study, the magnitudes of stresses in the substrate, graded layer, and the discrete stress jump across the substrate-100% NiCrAlY interface were lower than those predicted by our model (Fig. 2(a)). Based on finite element analysis, Baig et al.[28] demonstrated that for functionally graded magnesia stabilized zirconia+Ni coatings deposited on Nimonic alloy substrate, the compressive residual stress at the surface of the coating gradually becomes tensile with increasing distance from the surface into the coating.

4.1 Effect of number of layers

To show the effect of the number of layers we have considered the residual stress profiles for TBC systems S-1 and S-2 with the maximum YSZ volume fraction of 10%. The thicknesses of the bond coat and the top coat and were kept same. The maximum volume fraction of YSZ is also kept the same at 10% as before, and this YSZ content was the maximum concentration in systems with one, two, and 10 layers. For one layer, the entire 1.8 mm thick top coat consists of 10% YSZ and 90% of the bond coat material. For two layers, the top coat consists of two 0.9 mm thick layers with the first layer containing 5 vol.% YSZ and the next 0.9 mm thick layer

containing 10 vol.% YSZ. When the number of layers is increased to 10, the YSZ content was increased by 1% in each 0.18 mm thick layer. The stress profiles are plotted in Fig. 3(a) and 3(b).

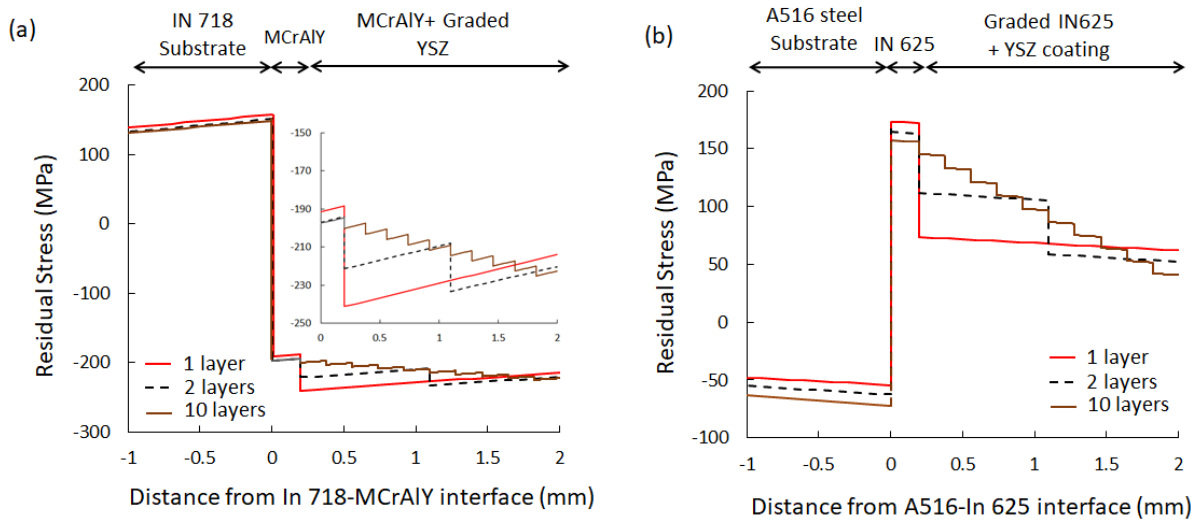

Figure 3: Residual stress profiles exhibiting the effect of the number of functionally graded layers for (a) IN 718-MCrAlY+YSZ (S-1) and (b) A516-IN 625+YSZ (S-2) TBC systems. The YSZ content increases in equal steps (10%/number of layers) up to a maximum at the top coat of 10 vol.% YSZ. The magnitude of discrete stress drops at the bond coat-top coat interface and through the top coat decreases with increasing the number of layers.

It is evident from Fig. 3(a) and Fig. 3(b) that the number of layers do not significantly influence the magnitude of stress in the substrate and the bond coat. But the magnitude of discrete stress drops at the bond coat-top coat interface and at the interfaces through the graded top coat decreases with increasing the number of layers. The inset of Fig. 3(a) shows that for S-1 the magnitude of stress drop at the MCrAlY bond coat-top coat interface reduces from 50 MPa to only 6 MPa with increasing the number of graded layers from one to 10. Similarly for S-2 (Fig. 3(b)), the magnitude of stress drop decreases from 100 MPa to 10 MPa with increasing the number of graded layers from one to 10. High differences in stress levels at the interfaces may cause cracking. Increasing the number of graded layers decreases the stress change at interfaces and thus may reduce interfacial cracking. Such a decrease in discrete stress levels with an

increasing number of FG layers was predicted by Zhang et al.[27] Based on a finite element model, Widjaja et al.[29] demonstrated that a graded ZrO_2 system with layers of Al_2O_3 lowers the residual stresses compared to a purely ZrO_2 system. Due to these reductions in stress levels at interfaces and within individual layers, it might be possible to deposit a thicker coating by resorting to a functionally graded approach.

4.2 Effect of YSZ volume fraction

A high volume fraction of YSZ in the top coat is often necessary to increase the insulative value of the thermal barrier. To observe the effect of the YSZ concentration on the stress profiles, we increase the maximum volume fraction of YSZ in the functionally graded layer to 60% and then apply our model to the TBC systems S-1 and S-2. The number of layers in the top coat was varied among one, two, and 10.

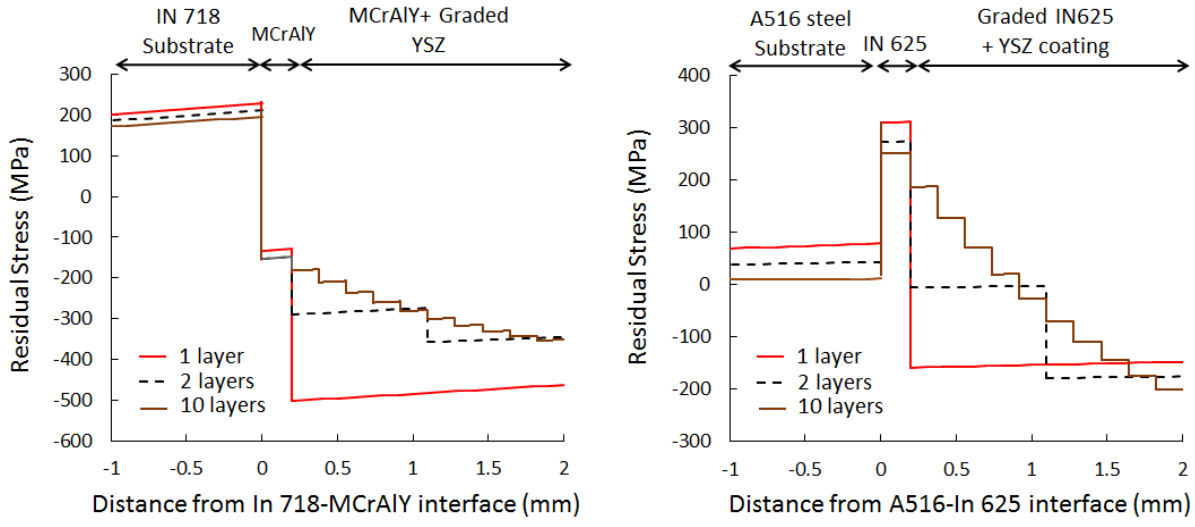

Figure 4: Residual stress profiles exhibiting the effect of number of functionally graded layers for (a) IN 718-MCrAlY+YSZ (S-1) and (b) A516-IN 625+YSZ (S-2) TBC system. The YSZ content increases in equal steps (60%/number of layers) up to a maximum at the top coat of 60 vol.% YSZ. The magnitude of discrete stress drops at the bond coat-top coat interface and through the top coat decreases with increasing the number of layers.

The stress profile for TBC system S-1 shown in Fig. 4(a) reveals that the magnitude of stress in the top coat, bond coat and substrate increases with increasing YSZ content. The top coat and substrate are under compression and tension, respectively. The magnitude of discrete stress drops at the interfaces is also greater as compared to that observed in Fig. 3(a). The magnitude of discrete stress drops at the interfaces are highest when the top coat consists of only a single layer of 40% MCrAlY+60% YSZ. Increasing the number of layers decreases the stress drops as explained in the last section. While -332 MPa (200 MPa to -132 MPa) of stress drop is predicted at the IN 718-MCrAlY interface, -374 MPa (-127 MPa to -502 MPa) of stress drop is predicted at the bond coat-top coat interface. The interfacial toughness of the bond coat-top coat interface for the single layer top coat is expected to be less than that of the substrate-bond coat interface. Therefore, the bond coat-TBC interface is prone to interfacial cracking due to the high magnitude of stress drop at that interface. However, the magnitude of stress drop decreases with increasing the number of layers, and hence the propensity of cracking may decrease.

The stress profile for the TBC system S-2 with maximum 60% YSZ is shown in Fig. 4(b) for one, two, and 10 layers. The basic nature of the profile is different from 10% YSZ shown in Fig. 3(b). In this case (Fig. 4(b)), the substrate and the bond coat are in tension. While the top coat may be either fully in compression, or be partially in compression as well as partially in tension, depends upon the number of graded layers. For a single layer (i.e. 40% IN 625+60% YSZ), the entire top coat is subjected to a compressive stress -154 MPa. However, a discrete stress drop of -467 MPa (308 MPa to -159 MPa)) is predicted at the bond coat-top coat interface (Fig. 4(b)), which may cause interfacial failure. Although increasing the number of layers decrease the sharp stress change across the interfaces, the bottom part of the top coat may be

subjected to tension and the stress state may change to compression at a distance further above the bond coat-top coat interface (Fig. 4(b)).

The TBC system may have finite curvature upon cooling as the layers are mutually bonded. There are two consequences of this which may impact component performance and lifetime. The warpage will cause loss of dimensional and shape conformance to specifications for the component. Further ceramics and ceramic-based materials, such as are used for TBCs, have low elastic limits and will thus be subject to premature failure. It is worthy of note that they exhibit greater strength in compression than in tension.

A finite curvature results due to a high coating to substrate thickness ratio of 0.157 in our study for the coating thickness of 2 mm and substrate thickness of 12.7 mm. The curvature effect gradually decreases with increasing the thickness of substrate and almost disappears when the film to substrate thickness ratio is less than 0.05 [30]. A similar effect was verified in our model.

The effect of the number of graded layers and the YSZ volume fraction on the curvature of a TBC system is shown in Fig. 5. It is evident from Figs. 5(a) and 5(b) that the curvatures of both TBC systems rapidly change when the number of top coat layers is increased from one to two. Increasing the number of layers beyond three has only a little effect on the curvature of the TBC system. The curvature of S-1 is always positive and is independent of the YSZ volume fraction at the top coat. Positive curvature results in compression of the top coat and tension in the substrate (Fig. 3(a) and 4(a)). In contrast the curvature of S-2 is negative when the YSZ volume fraction is low, which results in tensile stress in the top coat and compressive stress in the substrate. But with increasing the YSZ volume fraction in the top coat, the curvature of S-2

becomes positive. Therefore, a change in the stress state within the top coat, bond coat and substrate occurs in S-2 with increasing volume fraction of YSZ.

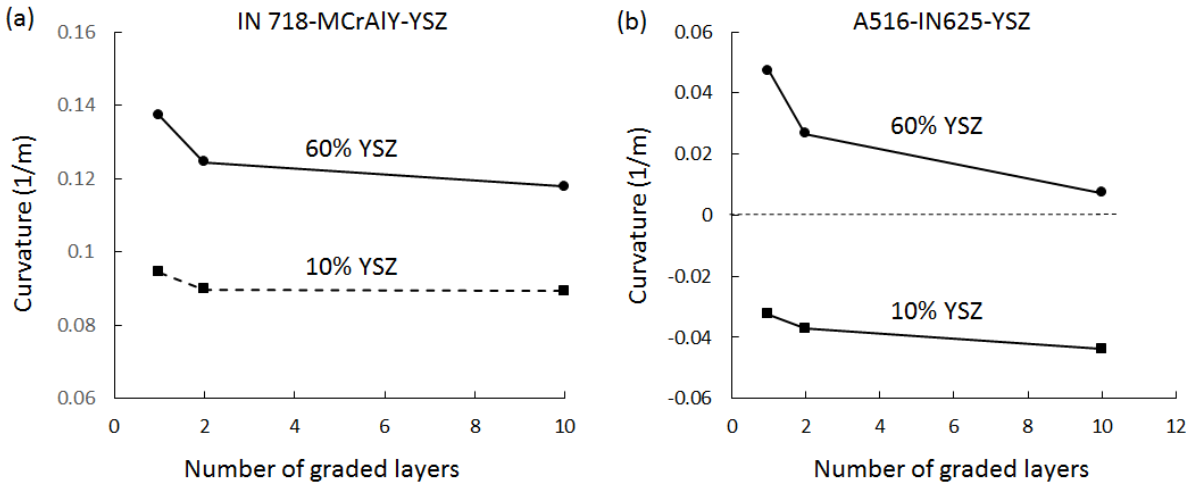

Figure 5: The effect of number of graded layers and volume fraction of YSZ in the top coat on the curvature of the TBC system (a) S-1 and (b) S-2. The thickness of substrate is 12.7 mm in both cases.

It is evident from Figs. 5(a) and 5(b) that the curvature of the coating system increases with increasing the degree of gradation (i.e. decreasing the number of layers and increasing the YSZ concentration at the top coat). The change in the curvature of the TBC systems is more pronounced at small numbers of layers and saturates as the number of layers increases. Figs. 5(a) and 5(b) reveals that the curvature saturates faster when the YSZ volume fraction is low. With increasing the thickness of the substrate, the curvature of the entire system decreases.

5. CONCLUSION

The curvature of the TBC system decreases with increasing the number of functionally graded layers in a TBC top coat. This may result in components failing to meet dimensional or shape specifications, or to premature failure of the ceramic-based TBC top coat. Although the magnitudes of stresses at the free surface of the substrate and the top coat are not influenced by the number of functionally graded layers, the magnitude of discrete stress variations at the interfaces reduces with increasing the number of layers. The stress state in the top coat depends significantly on the coefficient of thermal expansion of the substrate, bond coat and top coat. While the top coat is always in compression for the IN 718-NiCrAlY-NiCrAlY+YSZ system (S-1), the top coat can remain in tension or partially in tension and compression depending upon the YSZ concentration at the top coat. Increasing the YSZ concentration gradually changes the stress state of the top coat from fully in tension to partial tension at close proximity to the bond coat-top coat interface, and further to compression near the free surface of the top coat.

ACKNOWLEDGEMENTS

This technical effort was performed in support of the National Energy Technology Laboratory's ongoing gasification research, in the Advance Reaction Systems program. This research was also supported in part by an appointment to the National Energy Technology Laboratory Research Participation Program, sponsored by the U.S. Department of Energy and administered by the Oak Ridge Institute for Science and Education.

DISCLAIMER

This work was funded by the U.S. Department of Energy, National Energy Technology Laboratory, an agency of the United States Government.

1. INTRODUCTION

1. Clarke, D.R., M. Oechsner, and N.P. Padture, *Thermal-barrier coatings for more efficient gas-turbine engines.* MRS Bulletin, 2012. **37**(10): p. 891-898.
2. Wang, C.-L., et al., *Synthesis of Gadolinium Zirconate by Coprecipitaiton and Its Properties for TBC Application.* Key Engineering Materials, 2005. **280-283**: p. 1501-1502.
3. Saini, A.K., D. Das, and M.K. Pathak, *Thermal Barrier Coatings -Applications, Stability and Longevity Aspects.* Procedia Engineering, 2012. **38**: p. 3173-3179.
4. Liu, Z.-G., et al., *Novel thermal barrier coatings based on rare-earth zirconates/YSZ double-ceramic-layer system deposited by plasma spraying.* Journal of Alloys and Compounds, 2015. **647**: p. 438-444.
5. Evans, A.G., et al., *Mechanisms controlling the durability of thermal barrier coatings.* Progress in Materials Science, 2001. **46**(5): p. 505-553.
6. Taylor, R., J.R. Brandon, and P. Morrell, *Microstructure, composition and property relationships of plasma-sprayed thermal barrier coatings.* Surface and Coatings Technology, 1992. **50**(2): p. 141-149.
7. Lima, C.R.C. and J.M. Guilemany, *Adhesion improvements of Thermal Barrier Coatings with HVOF thermally sprayed bond coats.* Surface and Coatings Technology, 2007. **201**(8): p. 4694-4701.
8. Howe, J.M., *Bonding, structure, and properties of metal/ceramic interfaces: Part 1 Chemical bonding, chemical reaction, and interfacial structure.* International Materials Reviews, 1993. **38**(5): p. 233-256.

9. Howe, J.M., *Bonding, Structure and Properties of Metal/Ceramic Interfaces.* MRS Proceedings, 2011. **314**.
10. Cao, X.Q., R. Vassen, and D. Stoever, *Ceramic materials for thermal barrier coatings.* Journal of the European Ceramic Society, 2004. **24**(1): p. 1-10.
11. Cernuschi, F., et al., *Thermal diffusivity/microstructure relationship in Y-PSZ thermal barrier coatings.* Journal of Thermal Spray Technology, 1999. **8**(1): p. 102-109.
12. Levi, C.G., *Emerging materials and processes for thermal barrier systems.* Current Opinion in Solid State and Materials Science, 2004. **8**(1): p. 77-91.
13. Freund, L.B. and S. Suresh, *Thin film materials: stress, defect formation and surface evolution*. 2004: Cambridge University Press.
14. Bhattacharyya, A. and D. Maurice, *On the evolution of stresses due to lattice misfit at a Ni-superalloy and YSZ interface.* Surfaces and Interfaces, 2018. **12**: p. 86-94.
15. Hawa, H.A.E., A. Bhattacharyya, and D. Maurice, *Modeling of thermal and lattice misfit stresses within a thermal barrier coating.* Mechanics of Materials, 2018. **122**: p. 159-170.
16. Khor, K.A. and Y.W. Gu, *Effects of residual stress on the performance of plasma sprayed functionally graded ZrO2/NiCoCrAlY coatings.* Materials Science and Engineering: A, 2000. **277**(1): p. 64-76.
17. Kokini, K., et al., *Thermal shock of functionally graded thermal barrier coatings with similar thermal resistance.* Surface and Coatings Technology, 2002. **154**(2): p. 223-231.
18. Shaw, L.L., *Thermal residual stresses in plates and coatings composed of multi-layered and functionally graded materials.* Composites Part B: Engineering, 1998. **29**(3): p. 199-210.
19. Hou, P., S.N. Basu, and V.K. Sarin, *Structure and high-temperature stability of compositionally graded CVD mullite coatings.* International Journal of Refractory Metals and Hard Materials, 2001. **19**(4): p. 467-477.
20. Saul, R.H., *Effect of a GaAsxP1−x Transition Zone on the Perfection of GaP Crystals Grown by Deposition onto GaAs Substrates.* Journal of Applied Physics, 1969. **40**(8): p. 3273-3279.
21. Olsen, G.H. and M. Ettenberg, *Calculated stresses in multilayered heteroepitaxial structures.* Journal of Applied Physics, 1977. **48**(6): p. 2543-2547.
22. Liu, H.C. and S.P. Murarka, *Elastic and viscoelastic analysis of stress in thin films.* Journal of Applied Physics, 1992. **72**(8): p. 3458-3463.
23. Teixeira, V., *Mechanical integrity in PVD coatings due to the presence of residual stresses.* Thin Solid Films, 2001. **392**(2): p. 276-281.
24. Teixeira, V., *Residual stress and cracking in thin PVD coatings.* Vacuum, 2002. **64**(3): p. 393-399.
25. Mao, W.G., et al., *Modeling of residual stresses variation with thermal cycling in thermal barrier coatings.* Mechanics of Materials, 2006. **38**(12): p. 1118-1127.
26. Hsueh, C.H., *Thermal stresses in elastic multilayer systems.* Thin Solid Films, 2002. **418**(2): p. 182-188.
27. Zhang, X.C., et al., *Modeling of thermal residual stresses in multilayer coatings with graded properties and compositions.* Thin Solid Films, 2006. **497**(1): p. 223-231.
28. Baig, M.N., et al., *Properties and residual stress distribution of plasma sprayed magnesia stabilized zirconia thermal barrier coatings.* Ceramics International, 2014. **40**(3): p. 4853-4868.

29. Widjaja, S., A.M. Limarga, and T.H. Yip, *Modeling of residual stresses in a plasma-sprayed zirconia/alumina functionally graded-thermal barrier coating.* Thin Solid Films, 2003. **434**(1): p. 216-227.
30. Moridi, A., et al., *Residual stresses in thin film systems: Effects of lattice mismatch, thermal mismatch and interface dislocations.* International Journal of Solids and Structures, 2013. **50**(22): p. 3562-3569.